

Article

Not peer-reviewed version

Ambient Backscatter Based User Cooperation for mmWave Wireless Powered Communication Networks with Lens Antenna Arrays

[Rongbin Guo](#) , [Rui Yin](#) , Guan Wang , Congyuan Xu , [JianTao Yuan](#) *

Posted Date: 14 August 2024

doi: 10.20944/preprints202408.1066.v1

Keywords: ambient backscatter; user cooperation; WPCN; lens antenna array




Preprints.org is a free multidiscipline platform providing preprint service that is dedicated to making early versions of research outputs permanently available and citable. Preprints posted at Preprints.org appear in Web of Science, Crossref, Google Scholar, Scilit, Europe PMC.

Copyright: This is an open access article distributed under the Creative Commons Attribution License which permits unrestricted use, distribution, and reproduction in any medium, provided the original work is properly cited.

Article

Ambient Backscatter Based User Cooperation for mmWave Wireless Powered Communication Networks with Lens Antenna Arrays

Rongbin Guo ^{1,2} , Rui Yin ^{1,3}, Guan Wang ^{1,2}, Congyuan Xu ⁴ and JianTao Yuan ^{1,3*}

¹ College of Computer Science and Technology, Zhejiang University, Hangzhou 310058, China; rbguoieee@zju.edu.cn (R.G.); yinrui@hzcu.edu.cn (R.Y.); wangguan@hzcu.edu.cn (G.W.); cyxu@zjxu.edu.cn (C.Y.);

² School of Information and Electrical Engineering, Hangzhou City University, Hangzhou 310015, China;

³ Zhejiang Engineering Research Center of Building's Digital Carbon Neutral Technology, Hangzhou 310015, China

⁴ College of Information Science and Engineering, Jiaying University, Jiaying 314001, China;

* Correspondence: yuanjt@hzcu.edu.cn

Abstract: With the rapid consumer adoption of mobile devices such as tablets and smart phones, the tele-traffic has experienced a tremendous growth, low power technologies are highly desirable for future communication networks. In this paper, we consider an ambient backscatter (AB) based user cooperation (UC) scheme for mmWave wireless powered communication networks (WPCN) with lens antenna arrays. Firstly, we formulate an optimization problem to maximize the minimum rate of two users by jointly designing power and time allocation. Then we introduce auxiliary variables and transform the original problem into a convex form. Finally, we propose an efficient algorithm to solve the transformed problem. Simulation results demonstrate that the proposed AB based UC scheme outperforms the competing schemes, thus improve the fairness performance of throughput in WPCN.

Keywords: ambient backscatter; user cooperation; WPCN; lens antenna array

1. Introduction

1.1. Motivation

With the continuous evolution of wireless networks, the sixth-generation (6G) communication is expected to provide ubiquitous connectivity, ultrabroadband and integrated sensing and communication, which will enable many significant application scenarios such as internet of things (IoT), intelligent transportation, environmental monitoring and so on [1–3]. It is estimated that the number of global network terminals will reach 125 billion by 2030, and there will be as high as 100 IoT connections per cubic meter [4]. Limited by device size and deployment environment, some IoT devices are energy constrained. Therefore, in addition to enhancing the spectrum efficiency, low power technologies are highly desirable for future communication networks.

In this regard, wireless energy transfer (WET) relying on radio frequency (RF) transmission is a potential technology which provides sufficient power supply to energy constrained wireless systems. Moreover, the seamless combination of WET and wireless communication expands a hot research topic, i.e. wireless powered communication networks (WPCN) [5–7]. In WPCN, a harvest-then-transmit (HTT) protocol is proposed in [8], where the users first harvest energy from the RF signals broadcast by a hybrid access point (HAP) in the downlink (DL), and then transmit their information to the HAP in the uplink (UL). However, the users located far away from the HAP harvest much less energy than those close to the HAP, but have to consume more energy to transmit data back to the HAP, which is named as a “doubly near far” user unfairness problem. With consideration of the fairness issue, user cooperation (UC) is an effective approach, in which the user far from the HAP cooperate with its adjacent user to transmit signals to the HAP.

Several UC schemes for WPCN have been developed based on different models [9–11]. The authors in [9] design the optimal energy beamforming and time assignment to investigate the system

information transmission performance limit with two single-antenna users and a HAP. The authors in [10] consider a reconfigurable intelligent surface (RIS) assisted UC in a WPCN. Then they jointly optimize the transmit time and power allocations of the two users and the passive array coefficients on reflecting the wireless energy and information signal to maximize the common minimum throughput of the system. In [11], the authors jointly optimize time allocation, power allocation, and energy beamforming vectors to maximize the energy-efficiency (EE) in the scenario contains two UC users and separated power station and information receiver.

A major design issue of the existing user cooperation schemes is that the overhead consumed on information exchange between the collaborating users. Specifically, a new low-cost ambient backscatter communication (AmBC) technique [12] allows users to transmit information by passively backscattering environment RF signals, thus achieving device battery conservation. Compared with the HTT mode, the IoT devices operating in backscatter mode have lower power consumption [13]. In AmBC systems, a backscatter device (BD) leverages existing surrounding modulated ambient signals (generated from RF sources like Wi-Fi access points, TV towers or base stations from the cellular network) for communication [14]. The BD modulates the backscattered signal by switching between the two modes: a backscattering mode, when the BD antenna is short-circuited, and a transmission mode, when the BD antenna is open-circuited. These modes are used to indicate bit '0' and bit '1'. Typically, the backscatter receiver (BR) is equipped with an energy detector (ED) [15] to calculate the received power levels of AmBC signals and then mapping them to corresponding transmitted signals from the BD. Consequently, the AmBC system is energy efficient without active RF signal transmission and also spectrally efficient as it shares the spectrum of the ambient RF source. Actually, except for ambient backscatter (AB), there are two types of backscatter modes: the bistatic backscatter (BB) for which the RF emitter and BR could be separately deployed and the monostatic backscatter (MB) for which the RF emitter and BR are colocated [16]. Unlike the other two types, the device with the AB mode communicates by modulating and reflecting surrounding ambient signals thus does not require dedicated spectrum and energy [17].

However, ambient backscatter communication entails the dependence on unpredictable data traffic to provide the required excitation signal for the IoT devices that use backscattering. Hence, the WPCN systems need to provide active RF signals with energy-efficient technologies like mmWave multiple-input multiple-output (MIMO) communication, which has become a key candidate technology for future cellular networks due to the availability of large spectrum resources at higher frequencies and high energy efficiency with beamforming. In addition, mmWave technology is appropriate for various short-range wireless communication scenarios such as IoT due to its short wavelength and wide frequency band.

1.2. Related Work

The mmWave-based communication systems with WPCN has been attracted much attentions in the recent researches. In [18], the authors studied the WPT performance of mmWave band with a typical low-power device. Compared to the lower frequency, the WPCN in mmWave bands can provide a better energy transfer coverage with optimal parameters. Furthermore, the authors in [19] investigated the performance of WPT of a massive mmWave WPCN, and the simulation results demonstrated that the mmWave WPT gained superior efficiency than WPCNs with low frequency. The authors in [20] introduced a more practical non-linear energy harvesting model in massive mmWave WPCN system and analysed the potential performance of WPT. The beam outage probability and energy outage probability of mmWave WPCN was investigated in [21] with a random energy beamforming scheme, and the distribution of energy receivers was followed by the homogeneous Poisson point process (HPPP). Then the authors analysed the optimal performance of mmWave WPCN system. In [22], the authors jointly designed the transmit power, beamforming and power split coefficient for the optimization of transmission performance of the WPCN-based mmWave with the imperfect channel state information (CSI). By exploiting the advantages of multiple antennas, energy beamforming can

be adopt to transfer energy signals to all users in mmWave WPCN. However, the conventional fully digital beamforming schemes result in unaffordable costs in terms of power consumption and RF chains.

1.3. Our Contributions

In this paper, we consider an AB based UC scheme in mmWave WPCN with multi-antennas on the HAP. We equip HAP with a discrete lens array (DLA) [23], which reduces the complexity and cost of the RF hardware as well as improving the power budget due to the lens' energy-focusing capability [24]. In consideration of user fairness, we first formulate an optimization problem to maximize the minimum rate of two users by jointly designing power and time allocation. In order to solve this nonconvex problem, we then introduce auxiliary variables and transform the original problem into a convex form. Finally, we propose an efficient algorithm to solve this problem. Simulation results demonstrate that compared to conventional UC schemes based on active communication, the proposed passive AB based UC scheme can effectively enhance the throughput performance of energy-constrained devices in mmWave WPCN. As we know, this scenario has not been investigated.

1.4. Notation and Paper Organization

The rest of this paper is organized as follows. Section 2 presents the AB based UC system model and formulates the optimization problem. The proposed algorithm is developed in Section 3. In Section 4, we analyze the results of our experiments, and Section 5 concludes the paper.

Notation: In this paper, lower-case letter a_{ij} denotes the (i, j) -th element of matrix A . Upper-case and lower-case boldface letters A and a denote a matrix and a vector, respectively. A^T , A^H , $\|A\|_2$ and $\text{Tr}(A)$ represent the transpose, conjugate transpose, Frobenius norm and trace of matrix A , respectively. I_K is the $K \times K$ identity matrix and $E\{\cdot\}$ denotes the expectation operation.

2. System Model and Problem Formulation

We consider a mmWave WPCN consisting of one HAP and two single-antenna users (i.e., U_1 and U_2). The HAP is equipped with a DLA, comprising M_t antennas and one RF chain. The network topology is shown in Figure 1, without loss of generality, we assume these three nodes are placed in a straight line. The HAP has fixed power supply, while the two users need to harvest energy from the received signals broadcast by the HAP in the DL WET phase. The harvested energy is stored in an energy buffer (e.g., rechargeable battery), then the users transmit information in the UL wireless information transmission (WIT) phase.

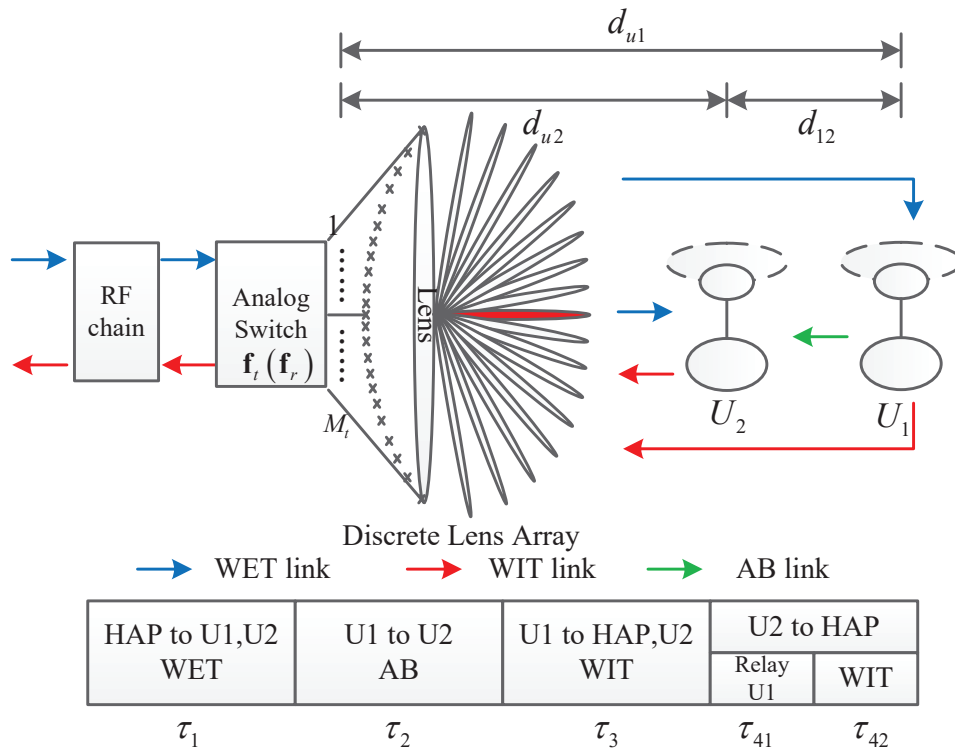


Figure 1. System model and transmission protocol for UC.

2.1. Channel Model

We assume that both WET and WIT operate over the same frequency band, and the channel reciprocity holds between the DL and UL. The beamspace channel matrix, $\tilde{\mathbf{H}}$, is transformed from the physical spatial MIMO channel:

$$\tilde{\mathbf{H}} = [\tilde{\mathbf{h}}_1, \tilde{\mathbf{h}}_2] = [\mathbf{U}\mathbf{h}_1, \mathbf{U}\mathbf{h}_2], \quad (1)$$

where $\mathbf{U} \in \mathbb{C}^{M_t \times M_t}$ is a discrete Fourier transformation (DFT) matrix corresponding to DLAs [23] at the HAP, $\mathbf{h}_k \in \mathbb{C}^{M_t \times 1}$ is the spatial domain channel vector between the HAP and user k . The DFT matrix \mathbf{U} consists of the array steering vectors of M_t orthogonal beams (directions) spread over the entire angular domain, i.e.:

$$\mathbf{U} = [\mathbf{a}(\varphi_1), \mathbf{a}(\varphi_2), \dots, \mathbf{a}(\varphi_{M_t})]^H, \quad (2)$$

where $\varphi_m = \frac{1}{M_t}(m - \frac{M_t+1}{2})$ with $m = 1, 2, \dots, M_t$ are the normalized spatial directions, $\mathbf{a}(\varphi_m) = \frac{1}{\sqrt{M_t}}(e^{-j2\pi\varphi_m i})_{i \in \mathcal{I}}$ are the corresponding $M_t \times 1$ array steering vectors, where $\mathcal{I} = \{i - (M_t - 1)/2 | i = 0, 1, \dots, M_t - 1\}$ is an index set of array elements.

Assuming transmission in a general multi-path environment, the channel can be written as:

$$\mathbf{h}_k = \beta_k^{(0)} \mathbf{a}(\phi_k^{(0)}) + \sum_{l=1}^L \beta_k^{(l)} \mathbf{a}(\phi_k^{(l)}), \quad (3)$$

the terms $\beta_k^{(0)} \mathbf{a}(\phi_k^{(0)})$ and $\beta_k^{(l)} \mathbf{a}(\phi_k^{(l)})$ represent the line-of-sight (LoS) and the l -th non-line-of-sight (NLoS) channel vectors between the HAP and user k , respectively. Furthermore, $\beta_k^{(0)}$ ($\beta_k^{(l)}$) denote the complex channel gains, while $\phi_k^{(0)}$ ($\phi_k^{(l)}$) represent the corresponding spatial directions. Here we only

consider the azimuth angles of departure (AoD)¹ for convenience, but the extension to a 3D scenario is straightforward and does not influence the feature of the problem. We assume that the beamspace channel matrix $\tilde{\mathbf{H}}$ is perfectly estimated by the HAP [24,25].

2.2. The Protocol Description

As shown in Figure 1, the system operates in four phases. In the first phase of duration τ_1 , the HAP transmits energy signal with the fixed power P_1 . The received energy signal at user k can be expressed as

$$y_{uk}^{(1)} = \sqrt{P_1} \tilde{\mathbf{h}}_k^H \mathbf{f}_t s_1 + n_{uk}, \quad (4)$$

in which s_1 satisfying $E\{s_1^H s_1\} = 1$ is the transmitted signal, $\tilde{\mathbf{h}}_k \in \mathbb{C}^{M_t \times 1}$ is the beamspace channel vector between the HAP and user k , $\mathbf{f}_t \in \mathbb{C}^{M_t \times 1}$ is the beam selection vector with only one non-zero element 1, $n_{uk} \sim \mathcal{CN}(0, \sigma_0^2)$ is the additive zero-mean circular complex Gaussian noise at user k , where σ_0^2 denotes the noise variance.

The HAP emits energy to all users with beam selection to improve WET. We select the beam with maximum magnitude [23] to transfer as much power as possible for each user. It is assumed that the energy harvested from noise n_{dk} can be neglected. Thus, the expected energy harvested by user k can be expressed as

$$E_{uk}^{(1)} = \eta P_1 \tau_1 |\tilde{\mathbf{h}}_k^H \mathbf{f}_t s_1|^2, \quad (5)$$

where the energy converting efficiency, $0 < \eta < 1$, is assumed fixed and equal for all users.

In the second phase with τ_2 amount of time, U_1 harvests energy from an incident signal transmitted by the HAP, and also backscatters different fraction of the incident signal to U_2 to transmit "0" or "1", respectively. In consequence, U_2 uses non-coherent detection techniques, e.g., energy detector [12], to decode the transmitted bit. If U_1 transmits a bit "0", U_2 receives only the energy signal from the HAP:

$$y_{u2,0}^{(2)} = \sqrt{P_1} \tilde{\mathbf{h}}_2^H \mathbf{f}_t s_2 + n_{u2}, \quad (6)$$

where s_2 satisfying $E\{s_2^H s_2\} = 1$ is the transmitted signal. On the other hand, when U_1 transmits a bit "1", U_2 receives combination of signals from both the HAP and U_1 , i.e.:

$$y_{u2,1}^{(2)} = \sqrt{P_1} \tilde{\mathbf{h}}_2^H \mathbf{f}_t s_2 + \mu \beta_{12} \sqrt{P_1} \tilde{\mathbf{h}}_1^H \mathbf{f}_t s_2 + n_{u2}, \quad (7)$$

where μ is the signal attenuation coefficient due to the reflection at U_1 , β_{12} denotes the channel coefficient between U_1 and U_2 .

We apply a power splitting scheme in U_2 , i.e., the received RF signal is split into two parts with a constant splitting factor $\gamma \in [0, 1]$. Accordingly, γ part of the RF signal power is harvested, and the rest $(1 - \gamma)$ part is used for information decoding (ID). The circuit of ID introduces an extra noise, $n_e \sim \mathcal{CN}(0, \sigma_1^2)$. We assume n_e is independent of n_{uk} , $k = 1, 2$. As a result, the signal at the ID receiver and energy decoder can be written as:

$$y_{u2,I}^{(2)} = \sqrt{1 - \gamma} y_{u2}^{(2)} + n_e, \quad y_{u2,E}^{(2)} = \sqrt{\gamma} y_{u2}^{(2)}, \quad (8)$$

¹ For simplicity, we assume that the elevation AoD is zero. This is practically valid if the separation distance between users and the HAP is much larger than their height difference.

where $y_{u2}^{(2)} = y_{u2,1}^{(2)}$ when U_1 backscatters "1", and $y_{u2}^{(2)} = y_{u2,0}^{(2)}$ when U_1 transmits "0". We assume that "0" and "1" are transmitted with equal probability without loss of generality. Then we can get the harvested energy by U_2 , which is given by:

$$\begin{aligned} E_{u2}^{(2)} &= \frac{1}{2} \eta \gamma \tau_2 (E[|y_{u2,1}^{(2)}|^2] + E[|y_{u2,0}^{(2)}|^2]) \\ &= \frac{1}{2} \eta \gamma P_1 \tau_2 (2|\tilde{\mathbf{h}}_2^H \mathbf{f}_t s_2|^2 + \mu^2 \beta_{12}^2 |\tilde{\mathbf{h}}_1^H \mathbf{f}_t s_2|^2). \end{aligned} \quad (9)$$

Note that here we assume the signal backscattered from U_1 is uncorrelated with the signal received directly from the HAP due to the random modulation during the backscatter phase. Besides, U_1 keeps its battery level unchanged, as the energy consumption on the operation of backscatter transmitter can be neglected due to the harvested energy during this phase. We also assume a fixed backscattering data rate R_b bps, and the sampling rate of backscatter receiver at U_2 is $N_b R_b$, which means the receiver takes N_b samples of each bit. We can get the bit error probability (BER) P_b of using an optimal energy detector to decode the received one-bit information: [15]

$$P_b = \frac{1}{2} \text{erfc} \left[\frac{(1 - \gamma) P_1 \mu^2 \sqrt{N_b} \beta_{12}^2 |\tilde{\mathbf{h}}_1^H \mathbf{f}_t s|^2}{4((1 - \gamma) \sigma_0^2 + \sigma_1^2)} \right]. \quad (10)$$

The communication process can be modeled as a binary symmetric channel, whose capacity is defined as bit per channel use, i.e.,

$$C_b = 1 + P_b \log P_b + (1 - P_b) \log(1 - P_b). \quad (11)$$

And the effective bit rate from U_1 to U_2 can be expressed as:

$$R_{12}^{(2)} = C_b R_b \tau_2. \quad (12)$$

In the third phase of duration τ_3 , U_1 transmits information to the HAP and U_2 simultaneously by exhausting the energy harvested in the first phase. The average transmit power of U_1 is given by

$$P_3 = E_{u1}^{(1)} / \tau_3 = \eta P_1 \tau_1 |\tilde{\mathbf{h}}_1^H \mathbf{f}_t s_1|^2 / \tau_3. \quad (13)$$

The received signal at the HAP and U_2 can be expressed as

$$y_{u0}^{(3)} = \sqrt{P_3} \mathbf{f}_r^T \mathbf{h}_1 s_3 + n_{u0}, \quad y_{u2}^{(3)} = \beta_{12} \sqrt{P_3} s_3 + n_{u2}, \quad (14)$$

where $\mathbf{f}_r^T \in \mathbb{C}^{1 \times M_t}$ is the beam selection vector which chooses the largest element of the UL channel \mathbf{h}_1 just like \mathbf{f}_t , s_3 satisfying $E\{|s_3|^2\} = 1$ is the complex base-band signal of U_1 , $n_{u0} \sim \mathcal{CN}(0, \sigma_0^2)$ denotes the receiver noise at HAP.

In the last phase, U_2 first transmits U_1 's signal to the HAP with power P_{41} and time τ_{41} , after that, U_2 transmits its own signal to the HAP with power P_{42} and time τ_{42} . We can obtain the total energy consumed by U_2 in the last phase constrained by the energy harvested in the first and second phase:

$$P_{41} \tau_{41} + P_{42} \tau_{42} \leq E_{u2}^{(1)} + E_{u2}^{(2)}. \quad (15)$$

We also have a total time constraint of time allocations $\boldsymbol{\tau} \triangleq (\tau_1, \tau_2, \tau_3, \tau_{41}, \tau_{42})$:

$$\tau_1 + \tau_2 + \tau_3 + \tau_{41} + \tau_{42} \leq T, \quad (16)$$

where T denotes the block duration in which the channel is static. Without loss of generality, we assume $T = 1$. Then the achievable rates of transmitting U_1 's signal from U_1 to U_2 and the HAP in the third phase, and from U_2 to the HAP in the last phase can be written as

$$R_{12}^{(3)} = \tau_3 \log_2 \left(1 + \frac{P_3 \beta_{12}^2}{\sigma_0^2} \right), \quad (17a)$$

$$R_{10}^{(3)} = \tau_3 \log_2 \left(1 + \frac{P_3 |f_r^T \mathbf{h}_1|^2}{\sigma_0^2} \right), \quad (17b)$$

$$R_{10}^{(4)} = \tau_{41} \log_2 \left(1 + \frac{P_{41} |f_r^T \mathbf{h}_2|^2}{\sigma_0^2} \right). \quad (17c)$$

Thus, the achievable rates of U_1 and U_2 within the duration $T = 1$ can be obtained [9]

$$R_1 = \min(R_{12}^{(2)} + R_{12}^{(3)}, R_{10}^{(3)} + R_{10}^{(4)}), \quad (18a)$$

$$R_2 = \tau_{42} \log_2 \left(1 + \frac{P_{42} |f_r^T \mathbf{h}_2|^2}{\sigma_0^2} \right). \quad (18b)$$

2.3. Problem Formulation

Under the max-min throughput criterion, we formulate the optimization problem by jointly designing power and time allocation of U_1 , U_2 and the HAP. The optimization problem can be formulated as

$$\max_{\mathbf{P}, \boldsymbol{\tau}} \min(R_1, R_2) \quad (19a)$$

$$\text{s.t. } \tau_1, \tau_2, \tau_3, \tau_{41}, \tau_{42} \geq 0, \quad (19b)$$

$$P_{41}, P_{42} \geq 0, \quad (19c)$$

$$(13), (15), (16), \quad (19d)$$

where $\mathbf{P} \triangleq (P_{41}, P_{42})$. Note that when we set $\tau_2 = 0$, the original problem (19) reduces to the case of a conventional UC scheme without AB. Furthermore, if we set $\tau_2 = \tau_{41} = 0$, (19) reduces to a case of WPCN without UC, which means the far user U_1 does not cooperate with the near user U_2 to transmit its information to the HAP.

3. Problem Transformation

Problem (19) is nonconvex due to the multiplicative terms in constraint (15), so we introduce auxiliary variables $\mathbf{V} \triangleq \{V_1, V_2\}$ satisfying $V_1 = P_{41} \tau_{41}$ and $V_2 = P_{42} \tau_{42}$ to deal with coupled variables $\{P_{41}, \tau_{41}\}$ and $\{P_{42}, \tau_{42}\}$. Then $R_{12}^{(3)}$ and $R_{10}^{(3)}$ in the original problem can be rewritten as functions of $\boldsymbol{\tau}$ and $\{V_1, V_2\}$. Besides, as P_3 is defined in (13), $R_{10}^{(4)}$ and R_2 can be re-expressed as functions of $\boldsymbol{\tau}$:

$$\begin{aligned} R_{12}^{(3)} &= \tau_3 \log_2 \left(1 + \frac{\delta_1 \tau_1}{\tau_3} \right), \\ R_{10}^{(3)} &= \tau_3 \log_2 \left(1 + \frac{\delta_2 \tau_1}{\tau_3} \right), \\ R_{10}^{(4)} &= \tau_{41} \log_2 \left(1 + \frac{V_1 \delta_3}{\tau_{41}} \right), \\ R_2 &= \tau_{42} \log_2 \left(1 + \frac{V_2 \delta_3}{\tau_{42}} \right). \end{aligned} \quad (20)$$

where

$$\begin{aligned}\delta_1 &= \frac{\eta P_1 \beta_{12}^2 |\tilde{\mathbf{h}}_1^H \mathbf{f}_{ts}|^2}{\sigma_0^2}, \\ \delta_2 &= \frac{\eta P_1 |\tilde{\mathbf{h}}_1^H \mathbf{f}_{ts}|^2 |\mathbf{f}_r^T \mathbf{h}_1|^2}{\sigma_0^2}, \\ \delta_3 &= \frac{|\mathbf{f}_r^T \mathbf{h}_2|^2}{\sigma_0^2}.\end{aligned}\quad (21)$$

are all constants. We also introduce an auxiliary variable R satisfying $R \leq \min(R_1, R_2)$. Then, we can transform the original problem (19) into an equivalent form expressed as

$$\max_{V, \tau} R \quad (22a)$$

$$\text{s.t. } R \leq R_{12}^{(2)} + R_{12}^{(3)}, \quad (22b)$$

$$R \leq R_{10}^{(3)} + R_{10}^{(4)}, \quad (22c)$$

$$R \leq R_2, \quad (22d)$$

$$V_1 + V_2 \leq E_{u2}^{(1)} + E_{u2}^{(2)}, \quad (22e)$$

$$\tau_1 + \tau_2 + \tau_3 + \tau_{41} + \tau_{42} \leq 1, \quad (22f)$$

$$\tau_1, \tau_2, \tau_3, \tau_{41}, \tau_{42} \geq 0. \quad (22g)$$

In which $R_{12}^{(3)}$, $R_{10}^{(3)}$, $R_{10}^{(4)}$ and R_2 are all concave functions. As $E_{u2}^{(1)}$ and $E_{u2}^{(2)}$ are affine functions of τ_1, τ_2 , we can find that problem (22) is convex, which can be addressed with existing convex optimization tools and algorithms, e.g. the CVX tool [26] and the interior point method. Finally, when we get the solution of (22), the optimal solution of \mathbf{P} can be obtained with $P_{41} = V_1 / \tau_{41}$ and $P_{42} = V_1 / \tau_{42}$.

4. Simulation Results

In this section, We consider a mmWave WPCN consisting of one HAP and two single-antenna users. The system configuration is defined by the following choice of parameters: the HAP is equipped with a DLA, comprising $M_t = 64$ antennas and one RF chain. Power of the HAP P_1 is set to 0 dBW. The noise power of all receivers σ_0^2 is set to -100 dBW, and the noise power of ID circuit σ_1^2 is set to -100 dBW. The energy converting efficiency $\eta = 0.6$. The power splitting factor of U_2 is $\gamma = 0.8$ and the signal attenuation coefficient is $\mu = 0.8$. We also choose two transmitting rates of AB for comparison, i.e., $R_b = 10$ Mbps and $R_b = 1$ Mbps, and the corresponding sample rate of AB is 6 times of R_b , i.e., $N_b = 6$. The channel model parameters are set as [27]: 1) one LoS link and $L = 2$ NLoS links; 2) $\phi_k^{(0)}$ and $\phi_k^{(l)}$ obey the uniform distribution within $[-\frac{1}{2}, \frac{1}{2}]$; 3) The LOS channel gain $(\beta_k^{(0)})^2 = G(\frac{c}{4\pi d_{uk} f_c})^2$, where $G = M_t$ is the antenna power gain, $c = 3 \times 10^8$ m/s is the speed of light, d_{uk} is the distance between user k and the HAP, $f_c = 30$ GHz is the carrier frequency of mmWave band. The channel gain between U_1 and U_2 is $(\beta_{12}^{(0)})^2 = G(\frac{c}{4\pi d_{12} f_c})^2$, where $d_{12} = d_{u1} - d_{u2}$ is the distance between U_1 and U_2 . We set the NLOS channel gain $\beta_k^{(l)} = 0.1\beta_k^{(0)}$.

In the rest of this section, we compare the max-min rate performance versus P_1 , M_t , d_{u1} and d_{u2} for different schemes, i.e., the AB based UC schemes with $R_b = 10$ Mbps and $R_b = 1$ Mbps (shown as $R_b = 1$ and $R_b = 10$ in simulaton results respectively), a UC scheme without AB (shown as "Without AB" in simulaton results), and a conventional scheme without UC (shown as "Without UC" in simulaton results). In Figure 2, we change the trasmitting power of the HAP P_1 from 1 W to 4 W. We can observe that the performances of all schemes are improved with increasing trasmitting power P_1 , and the proposed AB based UC schemes have better performance than other competing schemes.

The scheme with $R_b = 10$ has a better performance than the scheme with $R_b = 1$, which is owing to the higher R_b reduce more power consumption of information transmission between U_1 and U_2 .

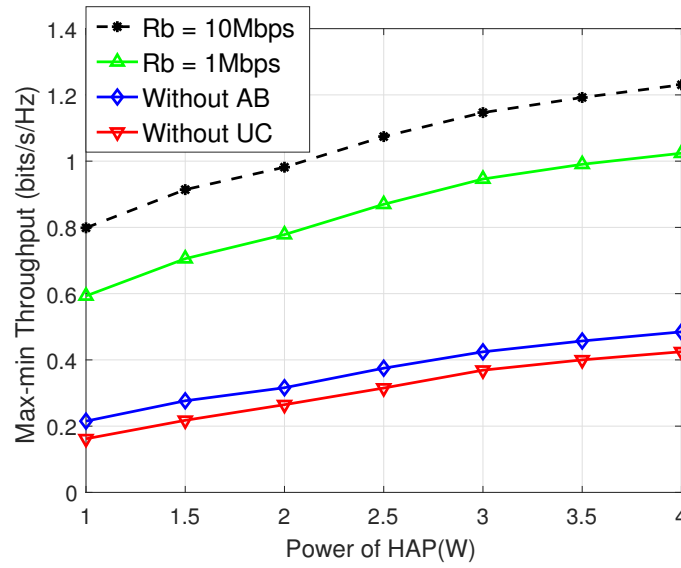


Figure 2. Performance of different schemes.

In Figure 3, we change the number of antennas at the HAP M_t from 8 to 64. We can observe that the performances of all schemes are improved with increasing number of antennas M_t which benefits from the energy capability of lens array. Similarly, the proposed AB based UC schemes have better performance than other competing schemes, which shows the AB technology can improve the performance of UC system.

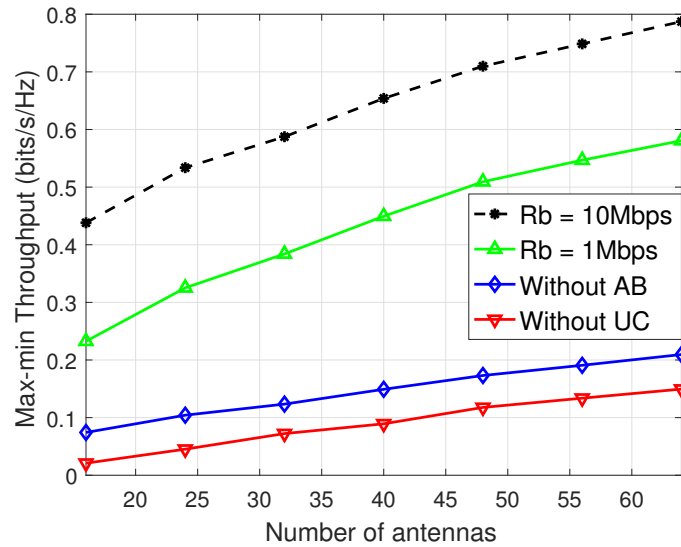


Figure 3. Performance of different schemes

In Figure 4, we set $P_1 = 4W$, $M_t = 64$ and $d_{u2} = 2$ m, and change d_{u1} from 4 m to 7 m. We can find that the performances of all schemes decrease when d_{u1} is getting longer, this is because the channel between U_1 and HAP attenuates more severely as d_{u1} increases. We can observe that the performance of AB based UC schemes decrease more slowly than other schemes, which means the use of passive AB can effectively reduce the energy consumptions and thus improve the throughput

performance. Hence, simulation results demonstrate the advantage of applying AB to improve the throughput performance of UC scheme in WPCN.

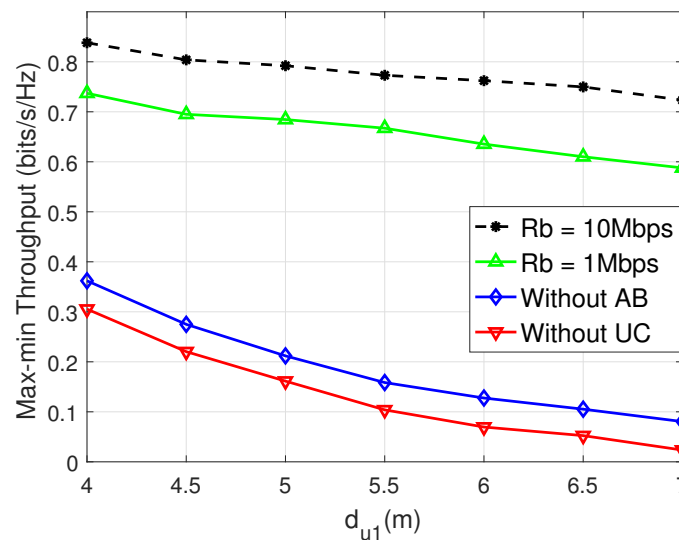


Figure 4. Performance of different schemes

In Figure 5, we set $P_1 = 4W$, $M_t = 64$ and $d_{u1} = 5$ m, and change d_{u2} from 1 m to 4 m. We can find that the performance of the scheme without UC hardly changes with d_{u2} , as its performance is mainly limited by the weak channel between the HAP and the farther user U_1 . On the other hand, the performances of AB based UC schemes increase when d_{u2} is getting shorter, this is because when d_{u2} decreases, the distance between U_1 and U_2 will increase, then U_1 needs more energy to transmit actively to the helping U_2 , and the use of passive AB can effectively reduce the energy consumptions and thus improve the throughput performance.

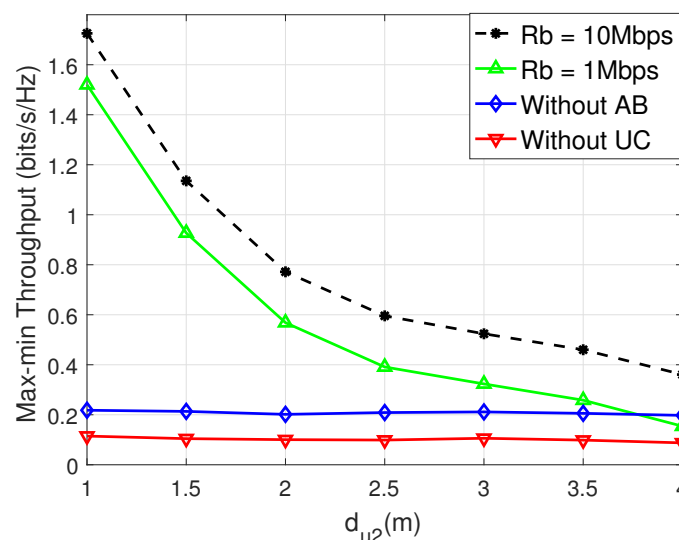


Figure 5. Performance of different schemes

5. Conclusions

In this paper, we have considered an AB based UC scheme in mmWave WPCN with lens antenna arrays. In particular, we have formulated an optimization problem to maximize the minimum rate of two users by jointly designing power and time allocation. After that, we have introduced auxiliary

variables and transformed the original problem into a convex form. Then we have proposed an efficient algorithm to solve the transformed problem. Simulation results have demonstrated that the AB based UC scheme outperforms the competing schemes, thus improved the throughput fairness performance in mmWave WPCN.

Author Contributions: Conceptualization: R.G., R.Y.; methodology: R.G., R.Y.; software: J.Y., C.X.; investigation: R.G., G.W., J.Y.; resources: R.G., R.Y.; data curation: J.Y., C.X.; writing—original draft preparation: R.G., J.Y.; writing—review and editing: R.G., R.Y.; visualization: R.G., G.W.; funding acquisition: R.G., R.Y. All authors have read and agreed to the published version of the manuscript.

Funding: This work was supported in part by the China Postdoctoral Science Foundation under Grant 2023M743063 and the Zhejiang Provincial Postdoctoral Scholarship under Grant ZJ2022107, in part by the National Natural Science Foundation of China under Grant 61771429, Grant 62302197 and Grant 62271438, Zhejiang Provincial Natural Science Foundation of China under Grant LQ23F020006.

Acknowledgments: The authors would like to thank the China Postdoctoral Science Foundation, the Zhejiang Provincial Postdoctoral Scholarship, National Natural Science Foundation of China (NSFC), Zhejiang Provincial Natural Science Foundation of China (ZPNSFC), Hangzhou City University and Zhejiang University for support this work.

Conflicts of Interest: The authors declare that there is no conflict of interests regarding the publication of this paper.

References

1. M. Latva-Aho and K. Leppanen, "Key drivers and research challenges for 6G ubiquitous wireless intelligence," Univ. Oulu, Oulu, Finland, White Paper 1, 2019. Available: <http://urn.fi/urn:isbn:9789526223544>
2. X. You et al., "Towards 6G wireless communication networks: Vision, enabling technologies, and new paradigm shifts," *Sci. China Inf. Sci.*, vol. 64, no. 1, pp. 1-74, 2021.
3. R. Guo, Y. Tang, C. Zhang, et al., "Prospects and Challenges of THz Precoding," *Chinese Journal of Electronics*, vol. 31, no. 3, pp. 488-498, 2022.
4. M. Alsabah et al., "6G Wireless Communications Networks: A Comprehensive Survey," *IEEE Access*, vol. 9, pp. 148191-148243, 2021.
5. Y. Zeng, B. Clerckx and R. Zhang, "Communications and signals design for wireless power transmission," *IEEE Trans. Commun.*, vol. 65, no. 5, pp. 2264-2290, May 2017.
6. G. Yang, Q. Zhang and Y. C. Liang, "Cooperative ambient backscatter communication systems for future internet-of-things," *IEEE Internet Things J.*, vol. 5, no. 2, pp. 1116-1130, Jan. 2018.
7. C. Yang, X. Wang and K. W. Chin, "On max-min throughput in backscatter-assisted wirelessly powered IoT," *IEEE Internet Things J.*, vol. 7, no. 1, pp. 137-147, Jan. 2020.
8. S. Zhong and X. Wang, "Transmission scheduling for hybrid backscatter-HTT nodes," *IEEE Internet Things J.*, vol. 8, no. 3, pp. 1769-1782, Feb. 2021.
9. X. Di, K. Xiong, P. Fan, H.-C. Yang, and K. B. Letaief, "Optimal resource allocation in wireless powered communication networks with user cooperation," *IEEE Trans. Wireless Commun.*, vol. 16, no. 12, pp. 7936-7949, 2017.
10. Y. Zheng, S. Bi, Y. J. Zhang, Z. Quan, and H. Wang, "Intelligent reflecting surface enhanced user cooperation in wireless powered communication networks," *IEEE Wireless Commun. Lett.*, vol. 9, no. 6, pp. 901-905, 2020.
11. A. M. Ahmed, Z. Wang, H. T. Belay and X. Wan, "Energy-Efficient Optimization for WPCN System Based on User Cooperation," in *2022 27th Asia Pacific Conference on Communications (APCC)*, Jeju Island, Korea, Republic of, pp. 329-333, 2022.
12. X. Lu, D. Niyato, H. Jiang, D. I. Kim, Y. Xiao and Z. Han, "Ambient backscatter assisted wireless powered communications," *IEEE Wireless Commun.*, vol. 25, no. 2, pp. 170-177, Apr. 2018.
13. Y. Zhuang, X. Li, H. Ji, H. Zhang and V. C. M. Leung, "Optimal resource allocation for RF-powered underlay cognitive radio networks with ambient backscatter communication," *IEEE Trans. Veh. Technol.*, vol. 69, no. 12, pp. 15216-15228, Dec. 2020.
14. Y. Zhuang, X. Li, H. Ji, and H. Zhang, "Exploiting hybrid SWIPT in ambient backscatter communication-enabled relay networks: Optimize power allocation and time scheduling," *IEEE Internet Things J.*, vol. 9, no. 24, pp. 24655-24668, Dec. 2022.

15. Z. Liu, S. Zhao, Y. Yang, K. Ma, and X. Guan, "Toward hybrid backscatter-aided wireless-powered Internet of Things networks: Cooperation and coexistence scenarios," *IEEE Internet Things J.*, vol. 9, no. 8, pp. 6264-6276, Apr. 2022.
16. C. Yang, X. Wang, and K.-W. Chin, "On max-min throughput in backscatter-assisted wirelessly powered IoT," *IEEE Internet Things J.*, vol. 7, no. 1, pp. 137-147, Jan. 2020.
17. Yunkai Hu, Peng Wang, Zihuai Lin, Ming Ding, Ying-Chang Liang, "Performance Analysis of Ambient Backscatter Systems With LDPC-Coded Source Signals," *IEEE Trans. Veh. Technol.*, vol. 70, no. 8, pp. 7870-7884, Aug. 2021.
18. T. A. Khan, A. Alkhateeb, and R. W. Heath, "Millimeter wave energy harvesting," *IEEE Trans. Wireless Commun.* Vol. 15, no. 9, pp. 6048-6062, Sep. 2016.
19. T. A. Khan and R. W. Heath, "Wireless power in millimeter wave tactical networks," *IEEE Signal Process. Lett.*, vol. 24, no. 9, pp. 1284-1287, Sep. 2017.
20. T. X. Tran, W. Wang, S. Luo, and K. C. Teh, "Nonlinear energy harvesting for millimeter wave networks with large-scale antennas," *IEEE Trans. Vehi. Technol.*, vol. 67, no. 10, pp. 9488-9498, Oct. 2018.
21. C. Psomas and I. Krikidis, "Energy beamforming in wireless powered mmWave sensor networks," *IEEE J. Sel. Areas Commun.*, vol. 37, no. 2, pp. 424-438, Feb. 2019.
22. G. Kwon, H. Park, and M. Z. Win, "Joint beamforming and power splitting for wideband millimeter wave SWIPT systems," *IEEE J. Sel. Topics Signal Process.*, vol. 15, no. 5, pp. 1211-1227, Aug. 2021.
23. R. Guo, Y. Cai, M. Zhao, Q. Shi, B. Champagne and L. Hanzo, "Joint Design of Beam Selection and Precoding Matrices for mmWave MU-MIMO Systems Relying on Lens Antenna Arrays," *IEEE J. Sel. Topics Signal Process.*, vol. 12, no. 2, pp. 313-325, May 2018.
24. R. Guo, Y. Cai, Q. Shi, M. Zhao and B. Champagne, "Joint design of beam selection and precoding for mmWave MU-MIMO systems with lens antenna array," in *Proc. IEEE 28th Annu. Int. Symp. Pers., Indoor, Mobile Radio Commun. (PIMRC)*, Oct. 2017, pp. 1-5.
25. S. Abeywickrama, C. You, R. Zhang and C. Yuen, "Channel Estimation for Intelligent Reflecting Surface Assisted Backscatter Communication," *IEEE Wireless Commun. Lett.*, vol. 10, no. 11, pp. 2519-2523, Nov. 2021.
26. CVX Research, Inc. CVX: Matlab software for disciplined convex programming, version 2.0 beta. [Online]. Available: <http://cvxr.com/cvx>
27. X. Gao, L. Dai, Z. Chen, Z. Wang, and Z. Zhang, "Near-optimal beam selection for beamspace mmWave massive MIMO systems," *IEEE Commun. Lett.*, vol. 20, no. 5, pp. 1054-1057, May 2016.

Short Biography of Authors



Rongbin Guo received the B.S. degree in Communication Engineering from Southwest Jiaotong University, Chengdu, China, in 2013, and the Ph.D degree in communication and information systems from Zhejiang University, Hangzhou, China, in 2018. From January 2019 to March 2022, he was an assistant professor with Research Center for Intelligent Network, Zhejiang Lab, Hangzhou, China. He currently holds a post-doctoral position at the School of Information and Electrical Engineering, Zhejiang University City College, Hangzhou, China and the College of Computer Science and Technology, Zhejiang University, Hangzhou, China. His research interests include B5G/6G communication systems, algorithm design for MIMO communication systems, and signal processing for wireless communications.



Rui Yin (M'13-S'19) received the B.E. degree in Computer Engineering from Yanbian University in 2001, China, the M.S. degree in Computer Engineering from KwaZulu-Natal University in Durban, South Africa in 2006, and the Ph.D. degree in Information and Electronic Engineering from Zhejiang University in 2011, respectively. From March 2011 to June 2013, he was a research fellow at the Department of Information and Electronic Engineering, Zhejiang University, China. He is now a professor in the School of Information and Electrical Engineering at Zhejiang University City College, China, and a joint honorary research fellow in the School of Electrical, Electronic and Computer Engineering at University of Kwa-Zulu Natal, South Africa. His research interests mainly focus on radio resource management in LTE unlicensed, millimeter wave cellular wireless networks, HetNet, cooperative communications, massive MIMO, optimization theory, game theory, and information theory. Prof. Yin regularly serves as the technical program committee (TPC) boards of prominent IEEE conferences such as ICC, GLOBECOM and PIMRC and chairs some of their technical sessions and reviewer for IEEE TWC, IEEE TVT, IEEE Tcom, IEEE Wireless Communications, IEEE Communications Magazine, IEEE Network, and IEEE TSP journals.

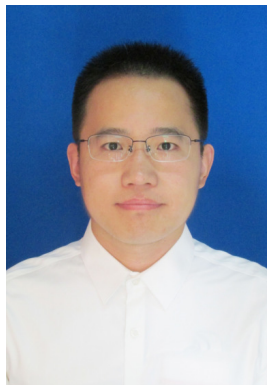


Guan Wang received his PhD in Computer Science and Technology from Zhejiang University in 2022. He is currently working as an assistant researcher at the School of Information and Electrical Engineering, Hangzhou City University, China. His research interests include engineering design, multi-objective optimization and uncertainty handling.



Congyuan Xu received the Ph.D. degree in Electronics Science and Technology from Zhejiang University, Hangzhou, China in 2019, and the B.S. degree in Applied Physics from Xidian University, Xi'an, China, in 2013. Currently, he is a lecturer in the College of Information Science and Engineering,

Jiaxing University, Jiaxing, China. His research interests focus on machine intelligence and cyberspace security.



Jiantao Yuan received the B.E. degree in electronic and information engineering from Dalian University, Dalian, China, in 2009, the M.S. degree in signal and information processing from The First Research Institute of Telecommunications Technology, Shanghai, China, in 2012, and the Ph.D. degree from the College of Information Science and Electrical Engineer, Zhejiang University, Hangzhou, China. He was with Datang mobile communication equipment co. LTD, Shanghai, China, from 2012 to 2013, where he was involved in LTE network planning and optimization. He used to work as a post-doctoral fellow at the Institute of Ocean Sensing and Networking of the Ocean College of Zhejiang University, Hangzhou, China, from 2019 to 2021. He is now working at School of Information and Electrical Engineering, Zhejiang University City College, Hangzhou, China. His research interests include cross-layer protocol design, 5G new-radio based access to unlicensed spectrum (NR-U), and ultra-reliable low latency communications (uRLLC).

Disclaimer/Publisher's Note: The statements, opinions and data contained in all publications are solely those of the individual author(s) and contributor(s) and not of MDPI and/or the editor(s). MDPI and/or the editor(s) disclaim responsibility for any injury to people or property resulting from any ideas, methods, instructions or products referred to in the content.